Title

Environmental chemical burden in metabolic tissues and systemic biological pathways in adolescent bariatric surgery patients: A pilot untargeted metabolomic approach

Authors

Valvi, Damaskini
Walker, Douglas I
Inge, Thomas
et al.

Publication Date

2020-10-01

DOI

10.1016/j.envint.2020.105957

Peer reviewed

HHS Public Access

Author manuscript

Environ Int. Author manuscript; available in PMC 2021 October 01.

Published in final edited form as:

Environ Int. 2020 October ; 143: 105957. doi:10.1016/j.envint.2020.105957.

Environmental chemical burden in metabolic tissues and systemic biological pathways in adolescent bariatric surgery patients: A pilot untargeted metabolomic approach

Damaskini Valvi, MD, PhD[1,*], **Douglas I. Walker, PhD**[1,*], **Thomas Inge, MD, PhD**[2], **Scott M Bartell, PhD**[3], **Todd Jenkins, PhD**[4], **Michael Helmrath, MD**[4], **Thomas R. Ziegler, MD**[5], **Michele A. La Merrill, PhD**[6], **Sandrah P. Eckel, PhD**[7], **David Conti, PhD**[7], **Yongliang Liang, MS**[8], **Dean P. Jones, PhD**[8], **Rob McConnell, MD**[7], **Leda Chatzi, MD, PhD**[7]

[1]Department of Environmental Medicine and Public Health, Icahn School of Medicine at Mount Sinai, New York, NY, United States

[2]Children's Hospital Colorado and University of Colorado, Denver, United States

[3]Program in Public Health and Department of Statistics, University of California, Irvine, CA, United States

[4]Cincinnati Children's Hospital and University of Cincinnati Departments of Pediatrics and Surgery, Cincinnati, OH, United States

[5]Division of Endocrinology, Metabolism and Lipids, Department of Medicine, Emory University School of Medicine; Atlanta, GA, United States

[6]Department of Environmental Toxicology, University of California, Davis, CA, United States

[7]Department of Preventive Medicine, University of Southern California, Los Angeles, CA, United States

[8]Clinical Biomarkers Laboratory, Department of Medicine, Emory University, Atlanta, GA, United States

Abstract

Contact information: Damaskini Valvi, MD MPH PhD, One Gustave L. Levy Place, Box 1057, New York, NY 10029, United States, Phone: +1 212-824-7062, dania.valvi@mssm.edu, Douglas I. Walker, PhD, One Gustave L. Levy Place, Box 1057, New York, NY 10029, United States, Phone: +1 212-824-7140, douglas.walker@mssm.edu.

*equal contribution

Author contributions: Conception and design of the study (D.V., D.I.W., R.M., L.C.); acquisition of data (D.I.W., T.I., T.J., M.H.); analysis of data (D.V., D.I.W.), interpretation of data (D.V., D.I.W., T.I., S.M.B., T.J., M.H., T.R.Z., M.A.L., S.P.E., D.C., Y.L., D.P.J., R.M., L.C.); drafting the article (DV, DIW); and critical revisions for important intellectual content (D.V., D.I.W., T.I., S.M.B., T.J., M.H., T.R.Z., M.A.L., S.P.E., D.C., Y.L., D.P.J., R.M., L.C.). D.V., D.I.W. and L.C. had primary responsibility for final content. All authors read and approved the final manuscript.

Conflicts of interest: The authors declare they have no conflict of interest, financial or otherwise.

Declaration of interests

The authors declare that they have no known competing financial interests or personal relationships that could have appeared to influence the work reported in this paper.

Background: Advances in untargeted metabolomic technologies have great potential for insight into adverse metabolic effects underlying exposure to environmental chemicals. However, important challenges need to be addressed, including how biological response corresponds to the environmental chemical burden in different target tissues.

Aim: We performed a pilot study using state-of-the-art ultra-high-resolution mass spectrometry (UHRMS) to characterize the burden of lipophilic persistent organic pollutants (POPs) in metabolic tissues and associated alterations in the plasma metabolome.

Methods: We studied 11 adolescents with severe obesity at the time of bariatric surgery. We measured 18 POPs that can act as endocrine and metabolic disruptors (i.e. 2 dioxins, 11 organochlorine compounds [OCs] and 5 polybrominated diphenyl ethers [PBDEs]) in visceral and subcutaneous abdominal adipose tissue (vAT and sAT), and liver samples using gas chromatography with UHRMS. Biological pathways were evaluated by measuring the plasma metabolome using high-resolution metabolomics. Network and pathway enrichment analysis assessed correlations between the tissue-specific burden of three frequently detected POPs (i.e. p,p'-dichlorodiphenyldichloroethene [DDE], hexachlorobenzene [HCB] and PBDE-47) and plasma metabolic pathways.

Results: Concentrations of 4 OCs and 3 PBDEs were quantifiable in at least one metabolic tissue for >80% of participants. All POPs had the highest median concentrations in adipose tissue, especially sAT, except for PBDE-154, which had comparable average concentrations across all tissues. Pathway analysis showed high correlations between tissue-specific POPs and metabolic alterations in pathways of amino acid metabolism, lipid and fatty acid metabolism, and carbohydrate metabolism.

Conclusions: Most of the measured POPs appear to accumulate preferentially in adipose tissue compared to liver. Findings of plasma metabolic pathways potentially associated with tissue-specific POPs concentrations merit further investigation in larger populations.

Keywords

persistent organic pollutants; adipose tissue; liver; bariatric surgery; exposome; high-resolution metabolomics

1. Introduction

Growing evidence supports the adverse metabolic effects of a wide list of substances that can interfere with hormonal action in animals and humans – the so-called "endocrine-disrupting chemicals (EDCs)" (Heindel et al. 2017; Ruiz et al. 2018). EDCs include persistent organic pollutants (POPs) with long-half lives in the human body (up to a decade) and lipophilic properties that promote their storage in fat-rich tissues. These POPs include dioxins, polychlorinated biphenyls (PCBs), organochlorine pesticides (e.g., dichlorodiphenyltrichloroethane [DDT]), and polybrominated diphenyl ethers (PBDEs) (Lee et al. 2014). Many epidemiologic studies have associated various POPs exposures with clinical markers for obesity and diabetes in adults and children (Burns et al. 2014; Cano-Sancho et al. 2017; Heindel et al. 2017; Iszatt et al. 2015; Karlsen et al. 2017; Lee et al. 2011; Lee et al. 2012; Lee et al. 2014; Ruiz et al. 2018; Vafeiadi et al. 2015; Vafeiadi et al.

2017; Valvi et al. 2012; Valvi et al. 2014; Valvi et al. 2017; Zong et al. 2018). However, there has been little study of underlying mechanisms in population studies, and previous association studies have almost exclusively measured POPs in peripheral blood.

Given the global epidemic trends of obesity, bariatric surgery is becoming an increasingly common intervention due to its demonstrated capacity to significantly reduce body weight and improve metabolic health indexes in adolescents and adults with severe obesity (Gletsu-Miller et al. 2009; Inge et al. 2016; Lin et al. 2009; Michalsky et al. 2018; Panunzi et al. 2016). However, there is large variability between individuals' metabolic responses to bariatric surgery, and the causes of this variability are relatively unknown (Ryder et al. 2019). POPs exposures may be one contributing factor, as recent studies show high concentrations of POPs in adipose tissue that are associated with adverse cardiometabolic profiles (Ferro et al. 2018) and attenuated weight loss in older patients after bariatric surgery (Pestana et al. 2014). However, this hypothesis is currently underexplored. The rich tissue repository of bariatric surgery cohorts provides a resource for addressing evidence gaps that cannot be easily addressed in general population studies, such as how POPs partition across different tissues. The repository also provides an opportunity to characterize biological mechanisms underlying POPs toxicity in key targeted metabolic tissues.

We conducted a feasibility study using state-of-the-art exposomic and metabolomic methods based upon ultra-high-resolution mass spectrometry (UHRMS) to characterize the burden of lipophilic POPs in metabolic (adipose and liver) tissues and associated biological pathways in peripheral blood. Findings can serve as a proof-of-concept for future investigations in bariatric surgery cohorts that aim to leverage a systems biology approach to provide insight into potential mechanisms underlying environmental toxicity in humans.

2. Methods

2.1 Study population and design

Eleven adolescents 12–20 years of age undergoing bariatric surgery at Cincinnati Children's Hospital between 2006 and 2012 were offered enrollment in a prospective biospecimen repository protocol (Pediatric Obesity Tissue Repository [POTR]). Sample recruitment and other POTR features have been reported previously (Davidson et al. 2017). Intraoperatively, visceral adipose tissue (vAT) samples from the omentum, abdominal subcutaneous AT (sAT), and liver samples were obtained by the surgeon and processed immediately in an area adjacent to the operating room. All samples were snap-frozen in liquid nitrogen, then stored at −80°C. Plasma was collected pre-operatively after overnight fasting and stored at −80°C. Written informed consent was obtained from participants equal to or above 18 years old or from the parent or guardian if participants were less than 18 years old. The study was approved by the Institutional Review Board at Cincinnati Children's Hospital.

2.2 Assessment of tissue-specific POPs concentrations

Targeted lipophilic POPs were selected due to prior evidence supporting their potentially adverse metabolic effects in animal and humans (Cano-Sancho et al. 2017; Heindel et al. 2017; Lee et al. 2014; Pestana et al. 2014; Ruiz et al. 2018). The 18 targeted POPs consisted

of two dioxins (2,3,7,8-tetrachlorodibenzo-p-dioxin [2,3,7,8-TCDD] and 2,3,7,8-tetrachlorodibenzofuran [2,3,7,8-TCDF]), 11 organochlorine compounds (OCs; including o,p'-dichlorodiphenyldichloroethene[DDE], p,p'-DDE, hexachlorobenzene [HCB], and eight PCB congeners (28, 52, 77, 101, 138, 153, 170, 180), and 5 PBDEs (congeners 28, 47, 99, 100 and 154). Limits of detection (LOD) varied across individuals based on POPs studied and the mass of available tissue (Table 1). Out of the 18 measured POPs, 7 (i.e. p,p'-DDE, HCB, PCB-28, PCB-153, PBDE-47, PBDE-100 and PBDE-154) had quantifiable concentrations above LOD in more than 80% of participants for at least one of the metabolic tissues, and therefore were included in subsequent statistical analysis. The percentages of values above LOD of the 11 POPs excluded from further analysis ranged from 0% to 64% in all three tissues (Supplementary Table S1).

Tissue POPs concentrations were measured in vAT, sAT and liver tissues collected during surgery. All tissue samples were prepared in batches of 11 study samples and 3 method blanks using a modified version of the QuECHERS method described by (Zamariola et al. 2017). Briefly, 0.2–0.5g of tissue was weighed, placed in an amber glass vial and treated with 3.5mL of LC-MS grade water. Each sample was then spiked with 50μL internal standard solution prepared in 2-proponal that was designed to represent environmental chemicals with a range of physiochemical properties to monitor analysis QA/QC, and included 500 ng/mL [$^{13}C_6$]-Anthracene, [$^{13}C_{12}$]-PCB28, [DIETHYL-D_{10}]-Chlorpyrifos, [$^{13}C_{12}$]-PCB101, [$^{13}C_{12}$]-4,4'-DDE, [$^{13}C_{12}$]-PCB153, [$^{13}C_{12}$]-PCB180, [$^{13}C_{12}$]-PBDE47, [$^{13}C_{10}$]-Mirex, [$^{13}C_6$]-cis-Permethrin, [$^{13}C_{12}$]-PBDE99 and [$^{13}C_{12}$]-PBB153. Following addition of the internal standard solution, the sample was then homogenized for 1 min and placed in a sonicating bath for 10 min. The resulting homogenate was transferred to a 50 mL conical tube containing 10mL acetonitrile, 4000mg $MgSO_4$ and1000mg NaCl, and vortexed for 5 min. After centrifuging, a 1.5mL aliquout was transferred to a cleanup tube containing 50 mg primary and secondary amine exchange material (PSA), 50 mg C_{18} and 150 mg $MgSO_4$, vortex-mixed for 1 min and centrifuged at max speed for 5 min. From the supernatant, a 1 mL aliquot was transferred to a clean, glass tube and dried completely in a vacuum centrifuge operated at 35°C. The residue was then resuspended in 50 μL isooctane and transferred to a GC vial containing a low volume insert and capped with a Teflon lined cap until analysis.

Tissue extracts were analyzed using a Thermo Scientific 1310 gas chromatograph connected to a Q Exactive GC Orbitrap GC-MS/MS ultra-high-resolution mass spectrometer and Triplus RSH autosampler. A 2 μL aliquot of extract was injected into an inlet maintained at 250ºC in pulsed split-less mode. The analytes were separated on an Agilent DB-5MSUI capillary column (30m length × 0.25mm inner diameter × 0.25μm film thickness) using high purity helium (99.999% purity) as the carrier gas at a constant flow rate of 1 mL/min. The oven temperature program consisted of an initial temperature of 100ºC for 1 min, increased to 180ºC at 25ºC/min; followed by a temperature ramp to 215ºC at 5ºC/min, and finally increased to 300ºC at 25ºC/min and held for 10 min, resulting in a total run time of 26.6 min. Analyte retention times were determined using individual standards and confirmed by matching analyte spectra to the 2014 National Institute of Standards and Technology mass spectral library.

Mass spectral data was obtained using an electron ionization source, operated at a source temperature of 250°C, electron impact energy of −70 eV and transfer line temperature maintained at 280°C. The UHRMS was operated in full-scan mode over mass-to-charge (*m/z*) range 85–850 and 60,000 resolution. Scan speed at this resolution was approximately 6 Hz, providing >12 scans across each peak. POPs concentrations were determined by comparison of the peak area of each analyte quantification ion to a 5-point calibration curve ranging from 0.1–10 ng/mL since ^{13}C internal standards were not available for all the quantified analytes. Only peaks within the analyte retention time +/− 0.2 minutes and exhibiting a qualifier ratio within 25% of the standard ratio were considered for quantification. The method detection limit was determined using the EPA method (USEPA [2003]) based upon repeated analysis (n=7) of the lowest spiking level. Raw GC-HRMS acquisition files and quantified POPs have been submitted to the Metabolomics Workbench (https://www.metabolomicsworkbench.org/; Study ID: ST001406; DOI: 10.21228/M86X2T).

2.3 Plasma high-resolution metabolomics

High-resolution metabolomics profiling was completed using well-established methods (Soltow et al. 2013). Samples were prepared and analyzed in a single batch and included four analyses of two separate pooled human plasma samples for quality control purposes. Plasma aliquots were removed from storage at −80°C, thawed and 50 μL was treated with 100 μL of ice-cold LC-MS grade acetonitrile. Plasma was then equilibrated for 30 min on ice, centrifuged (16.1 × *g* at 4°C) for 10 minutes to remove precipitated proteins, transferred to a 200 μL autosampler vial and maintained at 4°C until analysis (<22 h). Sample extracts were analyzed using liquid chromatography and Fourier transform high-resolution mass spectrometry (Dionex Ultimate 3000, Q-Exactive HF, Thermo Scientific). For each sample, 10 μL aliquots were analyzed in triplicate using hydrophilic interaction liquid chromatography with electrospray ionization source operated in positive mode. Analyte separation was accomplished by a 2.1 mm x 50 mm x 2.5 μm Waters XBridge BEH Amide XP hydrophilic interaction liquid chromatography and an eluent gradient (A= 2% formic acid, B= water, C= acetonitrile) consisting of an initial 1.5 min period of 2.5% A, 22.5% B, 75% C followed by a linear increase to 2.5% A, 77.5% B, 20% C at 4 min and a final hold of 1 min. Mobile phase flow rate was held at 0.35 mL/min for the first 1.5 min, increased to 0.5 mL/min and held for the final 4 min. The high-resolution mass spectrometer was operated at 120,000 resolution and mass-to-charge ratio (m/z) range 85–1275. Probe temperature, capillary temperature, sweep gas and S-Lens RF levels were maintained at 200°C, 300°C, 1 arbitrary units (AU), and 45, respectively. Additional source settings were optimized for sensitivity using a standard mixture, tune settings for sheath gas, auxiliary gas, sweep gas and spray voltage setting were 45 AU, 25 AU and 3.5 kV, respectively. Maximum C-trap injection times were set at 100 milliseconds and automatic gain control target 1×10^6. During untargeted data acquisition, no exclusion or inclusion masses were selected, and data was acquired in MS1 mode only. Raw data files were then extracted using apLCMS (Yu et al. 2009) at five different peak detection settings that have been separately optimized for detection of a wide range of peak intensities and abundances. Peaks detected during each injection were aligned using a mass tolerance of 5 ppm (parts-per-million) and retention grouping was accomplished using non-parametric density estimation grouping, with a

maximum retention time deviation of 30 seconds. The resulting feature tables were merged using xMSanalyzer, which identifies overlapping or unique features detected across the different peak detection parameters, and retains the peak with the lowest replicate CV and non-detects for inclusion in the final feature table (Uppal et al. 2013). All R-scripts for data extraction with apLCMS and data merging with xMSanalyzer are provided in the supplementary material. Uniquely detected ions consisted of *m/z*, retention time and ion abundance, referred to as *m/z* features. Prior to data analysis, triplicate *m/z* features averaged and filtered to remove those with triplicate coefficient of variation (CV) ≥ 100% and non-detected values greater than 10%. The final feature table included 14,144 *m/z* features with average triplicate CV of 30.7%. To further evaluate *m/z* feature quality, we assessed CV across replicate injections of the two separate pooled plasma samples. Mean CVs for *m/z* features detected in two or more injections for the two plasma pools were 29.9% and 31.7% for the 9,148 and 9,034 *m/z* features, respectively. Raw LC-HRMS acquisition files and processed feature tables have been submitted to the Metabolomics Workbench (Study ID: ST001407; DOI: 10.21228/M86X2T) and linked to GC-HRMS results (Project ID: PR000963).

2.4 Statistical analysis

Descriptive analysis included the comparison of mean POPs levels between tissue pairs using non-parametric Wilcoxon signed rank test, and the calculation of Spearman correlation coefficients (ρ) for within- and between-tissue POPs pairs. For the seven POPs included in the main analysis, values that were below LOD were substituted by LOD/2. All descriptive analyses were performed using R version 3.5.1.

For the integrated analysis of the tissue-specific POPs concentrations and the plasma metabolome, we initially visualized the relationships between different classes of POPs detected in each tissue type and in plasma metabolic alterations. We used a differential network analysis that tested for associations between the three POPs detected at the highest concentrations, including two OCs (i.e., p.p'-DDE, HCB) and one PBDE (i.e. PBDE-47), and the plasma metabolome. Network analysis was completed separately for POPs concentrations in each tissue using xMWAS (Uppal et al. 2018), which provides an automated framework for integrative and differential network analysis. Pairwise integration was first completed using partial least squares (Le Cao et al. 2009). The igraph package in R was then used to generate a multi-data integrative network (Casardi 2006), with only associations where $|r|>0.3$ and $p<0.05$ retained in the network. Metabolite and exposure clusters were identified in the network by the multilevel community detection method (Blondel et al. 2008), followed by determination of eigenvector centrality measure to compare the importance of nodes across the three tissues (Lichtblau et al. 2017). Enriched metabolic pathways were characterized using Mummichog (Li et al. 2013), which uses a permutation-based framework that accounts for the many-to-many mappings of *m/z* features and accounts for the additional complexity of untargeted mass spectral data while isolating biological effects and reducing type I error metabolites. When possible, metabolites annotated using Mummichog were compared using *m/z* and retention time to a database of confirmed endogenous compounds analyzed on the same system. Metabolite annotation confidence were reported using Schymanski et al. 2014 (Supplementary Tables S2–S4).

3. Results

The 11 adolescent bariatric surgery patients had a mean age (range) of 17 (11–20) years, who predominantly were females (n=10 vs 1 male) and of Caucasian origin (n=10 vs 1 African-American). All participants had severe obesity (body mass index in kg/m^2: mean [range] = 51 [36, 68]) and none of the participants were diagnosed with type 1 or 2 diabetes mellitus at the time of the surgery.

POPs with good detection rates (>80%) in at least one metabolic tissue included 4 OCs (p,p'-DDE, HCB, PCB-28 and PCB-153) and 3 PBDEs (congeners 47, 100 and 154) (Table 1). Among all POPs examined, p,p'-DDE was detected at the highest concentration in vAT (median[IQR]=5645 [3997–6263] pg/g-tissue) and in sAT (9170 [6433–13810] pg/g-tissue), whereas PBDE-154 was detected in the highest concentration in liver. Overall, all POPs had the lowest concentrations in the liver compared to adipose tissue compartments, except PBDE-154 for which concentrations did not significantly differ on average between tissues (median[IQR] in pg/g-tissue=1096 [435–1810] in vAT vs. 1311 [891–2347] in sAT vs. 1783 [750–2668] in liver; p-value = 0.18 for vAT-sAT difference, 0.79 for vAT-Liver, and 0.59 for sAT-Liver). Between adipose tissue types, except for PBDE-154, all other POPs were detected at higher concentrations in sAT than in vAT (p-value<0.05) (Table 1).

Between-tissue correlations using non-parametric Spearman ρ were significant for all pairwise comparisons of POPs examined (p-value<0.05) and, overall, were more modest for liver-adipose tissue POPs pairs ($-0.17 \leq \rho \leq 0.58$) and stronger for vAT-sAT POPs pairs ($0.17 \leq \rho \leq 0.89$) (Figure 1). Within-tissue correlations ranged from 0 to moderately high (Spearman $\rho = |0.80|$, depending on the POPs pair and tissue examined (Figure 1).

To identify systemic metabolic alterations associated with tissue-specific POPs concentrations, we used a network-based MWAS approach that tested for metabolic pathway alterations present in metabolite clusters associated with p,p'-DDE, HCB and PBDE-47 in each tissue. For all three tissues, POPs levels were correlated with alterations in metabolic features and pathways (Figures 2–3). Clustering of metabolites associated with vAT POPs suggests different biological response profiles were present for each POP, with three separate clusters for each exposure. Of these, HCB in vAT compared to other tissues showed the greatest number of correlated plasma pathways, including branched chain amino acids (BCAA), sulfur and other amino acid pathways, pathways of carbohydrate, microbial, nucleotide and nucleoside and co-factor metabolism. p,p'-DDE and PBDE-47, which were present in separate clusters in vAT, were correlated with xenobiotic metabolism and aspartate/asparagine, respectively.

For POPs levels in sAT and metabolite associations, we found two separate clusters, including one cluster centered on HCB and a second cluster that included p,p'-DDE and PBDE-47 (Figures 2–3). Both clusters included alterations in glycolysis and glucogenesis. Additional pathways associated with HCB included amino acid, lipid and fatty acid, and carbohydrate metabolism pathways, microbial, xenobiotic and Co-factor metabolism. The cluster of metabolites associated with p,p'-DDE and PBDE-47 in sAT included mainly lipid and carbohydrate metabolism pathways.

Metabolites associated with liver POPs were also present in two separate clusters, and were consistent with different pathways (Figures 2–3). HCB, which was present in one cluster, included alterations in lipid and fatty acid metabolism pathways, and amino acids, such as tryptophan metabolism. Liver p,p'-DDE and PBDE-47, which were present in the second cluster of metabolites, showed pathways from amino acid metabolism, including BCAA, microbiome-related pathways and nucleotide metabolism.

4. Discussion

We demonstrated the feasibility of quantifying a large number of POPs in multiple metabolic tissues, utilizing a rich bariatric surgery repository and state-of-the-art '-omics' technologies. We found large differences in POPs concentrations across metabolic tissues, and we observed higher concentrations accumulated in adipose tissue, especially in sAT, than in liver, for all POPs except PBDE-154, which had similar average concentrations across all tissues. Findings from this pilot study provide a proof-of-concept that multiple plasma metabolic pathways could be associated with tissue-specific POPs burden. The findings are relevant to the design of planned future investigations in larger populations with longitudinal follow-up of bariatric surgery patients. Such studies could provide mechanistic insight into findings from epidemiologic studies in which peripheral blood is the only available matrix for chemical profiling.

We measured many tissue POPs, including legacy dioxins, OCs including insecticides (DDT and HCB) and industrial byproducts (PCBs), and flame retardants (PBDEs). Although regulations have banned the use of OCs and restricted the use of PBDEs in the United States, we found detectable levels for almost all POPs in at least some study subjects' adipose and liver tissues. Only a few studies have assessed POPs partitioning across metabolic tissues in humans (Helaleh et al. 2018; Kim et al. 2014; Kim et al. 2011; Pestana et al. 2014), and no previous study has evaluated the associations between the tissue-specific POPs burden and the plasma metabolome.

We observed higher POPs concentrations in sAT compared to vAT tissue for almost all POPs examined, which is only partially consistent with findings from previous studies. A Portuguese adult bariatric surgery population, also largely female (89%), found higher concentrations of HCB in sAT, but lower concentrations of p,p'-DDE in sAT, compared to vAT concentrations (Pestana et al. 2014). Another recent study measured PBDEs in sAT and omental vAT collected from 34 predominantly female obese Qatari adults; higher concentrations of PBDE-154 were found in sAT compared to vAT, but lower concentrations of PBDE-47 were found in sAT (Helaleh et al. 2018). In our study we observed higher median concentrations in sAT compared to vAT for PBDE-47. It is possible that differences in lifetime exposures to POPs, based on population characteristics, may explain the higher accumulation in vAT compared to sAT reported among older patients for some POPs (Kim et al. 2014), in contrast to findings in our adolescent patient study. The higher concentrations seen in sAT compared to vAT for most OCs in the our study could also be due to physiological differences in sAT versus vAT, which may include lipid composition differences across adipose tissue compartments (Bourez et al. 2012)(Garaulet et al. 2001).

We found lower concentrations of all POPs in liver compared to adipose tissue, except for PBDE-154, which could be a chance finding, or it might suggest a more facilitated transport into, or slower metabolism or release rate of PBDE-154 from hepatocytes compared to other POPs (Hakk et al. 2009). At least one other study in humans has reported higher concentrations of PBDE-154 and some other PBDE congeners in liver than in adipose tissue, albeit in a small number of participants (Meironyte Guvenius et al. 2001). For other POPs, the lipophilicity and physico-chemical properties can explain the higher concentrations in the adipose tissue compared to the liver, as adipose is the main storage depot for accumulative exposures for most POPs (Jackson et al. 2017).

In our analysis of untargeted plasma metabolomics, we found evidence that some plasma metabolic pathways could be common for the different POPs examined and linked to the same POP exposure in all three metabolic tissues, while other metabolic pathways where unique to the POP exposure and tissue examined. For example, HCB and PBDE-47 or p,p'-DDE (examined either as a cluster exposure group, or separately) in both adipose tissue and liver were consistently correlated with aspartate and asparagine metabolism. To the contrary, pathways of lipid and fatty acid metabolism (i.e. de novo fatty acid biosynthesis and fatty acid activation) were shown to correlate only with HCB levels in sAT and liver, but not in vAT, and were not correlated with the other POPs in any tissue. The pathway of glycolysis and glyconeogenesis was shown to correlate with POPs exposures in sAT but not in vAT or liver. These preliminary findings suggest only a partial overlap of mechanisms of toxicity of different POPs in metabolic tissues.

HCB levels from both sAT and vAT were associated with BCAA metabolism (valine, leucine and isoleucine degradation), while PBDE-47 and p,p'-DDE levels in the liver were associated with this pathway. BCAAs, which provide a key signaling pathway that regulates functions related to energy homeostasis, nutrition metabolism and gut health, have previously been identified in a number of metabolomic studies as an early marker of insulin resistance and type 2 diabetes risk (Lynch and Adams 2014; Nie et al. 2018; Zhao et al. 2016). Thus, potential associations with altered BCAA metabolism and subsequent molecular effects could provide one possible mechanism explaining metabolic effects of POP exposures.

Alterations in pathways of lipid and fatty acid and carbohydrate metabolism have also been suggested by few previous metabolomic studies of POPs exposure. In a study of blood levels of HCB, p,p'-DDE, PCBs and hexachlorohexane, comparison of low and high exposure groups identified a series of metabolites identified as glycerophospholipids and sphingolipids associated with exposure (Carrizo et al. 2017). Similar findings were observed in a study of 1,016 elderly participants in Sweden (Salihovic et al. 2015), as well as using an untargeted metabolomic approach in a US population with elevated dietary exposures to OCs and brominated flame retardants (Walker et al. 2019). These metabolomic findings are consistent with previous results that have shown PCBs can reduce synthesis of long-chain unsaturated fatty acids by inhibiting delta 5 and delta 6 desaturase activities in the liver (Matsusue et al. 1999). MWAS of plasma levels of DDT and degradation products during pregnancy and early postpartum also showed p,p'-DDE was associated with changes in multiple fatty acid and lipid pathways (Hu et al. 2019). Taken together, these results suggest

exposure to lipophilic POPs leads to disruption in essential fatty acid metabolism and related glycolytic and lipid pathways, which may have important implications for fatty liver and other metabolic diseases (Murphy et al. 2015; Scorletti and Byrne 2013).

An important study limitation is the small sample size, which reduced power and could explain some inconsistencies in pathway associations across POPs and tissues. We also limited our analyses to bariatric surgery patients with extreme obesity who provided a unique resource of samples from metabolic tissues that cannot be easily accessible in healthy subjects, and therefore our results may not be fully generalizable to the general population or to lean subjects. Due to the small sample we provided results for the POPs-metabolome analysis unadjusted for important confounders, such as age, sex, preoperative weight loss, and diet patterns and composition. Diet is an important source of exposure to POPs for the general population (Arrebola et al. 2012; Frederiksen et al. 2009; Linares et al. 2010) and dietary macronutrient composition may also influence the POP accumulation in metabolic tissues (Myrmel et al. 2016). Association studies with proper adjustment for confounders are required in larger populations with available metabolic tissue samples to draw valid causal inferences. Prospective study designs are particularly needed to exclude reverse causation as an explanation for our findings, as weight gain, preoperative weight loss, and altered metabolic pathways in severely obese subjects could influence the uptake and elimination of lipophilic POPs in metabolic tissues (Imbeault et al. 2002; Wolff et al. 2005). POPs reflect chronic exposure, while metabolic pathways may reflect short-term effects of other covariates. Prospective investigations with repeated measures of untargeted high-resolution metabolomics could help address uncertainty in the temporal variability of some metabolites that has not been extensively studied (Carayol et al. 2015; Floegel et al. 2011). Future investigations of tissue-specific POPs concentrations should include lipid adjusted POP measures and complement exposure assessment with POP concentrations in plasma. Important study strengths include the bariatric surgery design that provided a rich tissue repository for the characterization of the POPs burden in metabolic tissues including the liver. Innovative high-resolution metabolomics technologies allowed us to evaluate for the first time the correlations between the tissue-specific POPs concentrations and plasma metabolic pathways. Findings pointed to many metabolic pathways potentially altered by POPs, which requires further investigation in prospective studies and larger populations.

5. Conclusions

Using state-of-the-art exposomic and metabolomic methods, we showed greater concentrations of POPs in adipose tissue compared to liver for all POPs examined, except PBDE-154. The tissue-specific POPs concentrations were correlated with multiple plasma metabolic pathways, including amino acid metabolism, lipid and fatty acid metabolism, and carbohydrate metabolism. Findings provide complementary insight to previous investigations where peripheral blood was the only available matrix for chemical profiling and can inform the design of future investigations in bariatric surgery cohorts that aim to leverage a systems biology approach for insight into potential mechanisms underlying environmental toxicity in humans.

Supplementary Material

Refer to Web version on PubMed Central for supplementary material.

Acknowledgments:

The authors are grateful to the Pediatric Obesity Tissue Repository (POTR) participants for their generous collaboration. We are grateful to Jennifer Black, Study Coordinator for her generous assistance in getting access to the POTR repository. This study was supported by the National Institute of Health, the National Institute of Environmental Health Sciences (R21ES028903, R21ES029328, R21ES029681, R01ES029944, R01ES030364, R01ES024946, U2CES026561, U2CES030163, P30ES023515, P30ES019776, P30ES007048, P01ES022845, R01ES024946, R01ES030691), USDA National Institute of Food and Agriculture (Hatch project: 1002182), and the U. S. Environmental Protection Agency (RD-83544101).

Abbreviations:

AU	Arbitrary units
BCAA	Branched chain amino acid
DDE	Dichlorodiphenyldichloroethene
DDT	Dichlorodiphenyltrichloroethane
EDCs	Endocrine-disrupting chemicals
HCB	Hexachlorobenzene
LOD	Limits of detection
MWAS	Metabolome wide association study
OCs	Organochlorine compounds
PBDE(s)	polybrominated diphenyl ether(s)
PCB(s)	Polychlorinated biphenyl(s)
POP(s)	Persistent organic pollutant(s)
POTR	Pediatric obesity tissue repository
sAT	subcutaneous adipose tissue
UHRMS	Ultra-high-resolution mass spectrometry
vAT	Visceral adipose tissue
2,3,7,8-TCDD	2,3,7,8-tetrachlorodibenzo-p-dioxin
2,3,7,8-TCDF	2,3,7,8-tetrachlorodibenzofuran

References

Centers for Disease Control and Prevention. 2019 Fourth national report on human exposure to environmental chemicals - Updated tables, January 2019. Available: https://www.cdc.gov/exposurereport/index.html [accessed June 5 2019].

Arrebola JP, Mutch E, Rivero M, Choque A, Silvestre S, Olea N, et al. 2012 Contribution of sociodemographic characteristics, occupation, diet and lifestyle to ddt and dde concentrations in serum and adipose tissue from a bolivian cohort. Environ Int 38:54–61. [PubMed: 21982033]

Blondel VD, Guillaume JL, Lambiotte R, Lefebvre E. 2008 Fast unfolding of communities in large networks. J Stat Mech-Theory E.

Bourez S, Le Lay S, Van den Daelen C, Louis C, Larondelle Y, Thome JP, et al. 2012 Accumulation of polychlorinated biphenyls in adipocytes: Selective targeting to lipid droplets and role of caveolin-1. PLoS One 7:e31834. [PubMed: 22363745]

Burns JS, Williams PL, Korrick SA, Hauser R, Sergeyev O, Revich B, et al. 2014 Association between chlorinated pesticides in the serum of prepubertal russian boys and longitudinal biomarkers of metabolic function. Am J Epidemiol 180:909–919. [PubMed: 25255811]

Cano-Sancho G, Salmon AG, La Merrill MA. 2017 Association between exposure to p,p'-ddt and its metabolite p,p'-dde with obesity: Integrated systematic review and meta-analysis. Environmental health perspectives 125:096002. [PubMed: 28934091]

Carayol M, Licaj I, Achaintre D, Sacerdote C, Vineis P, Key TJ, et al. 2015 Reliability of serum metabolites over a two-year period: A targeted metabolomic approach in fasting and non-fasting samples from epic. PLoS One 10:e0135437. [PubMed: 26274920]

Carrizo D, Chevallier OP, Woodside JV, Brennan SF, Cantwell MM, Cuskelly G, et al. 2017 Untargeted metabolomic analysis of human serum samples associated with exposure levels of persistent organic pollutants indicate important perturbations in sphingolipids and glycerophospholipids levels. Chemosphere 168:731–738. [PubMed: 27825712]

Casardi G 2006 The igraph software package for complex network research. InterJournal; Complex Systems:1695.

Davidson WS, Inge TH, Sexmith H, Heink A, Elder D, Hui DY, et al. 2017 Weight loss surgery in adolescents corrects high-density lipoprotein subspecies and their function. Int J Obes (Lond) 41:83–89. [PubMed: 27780977]

Ferro A, Teixeira D, Pestana D, Monteiro R, Santos CC, Domingues VF, et al. 2018 Pops' effect on cardiometabolic and inflammatory profile in a sample of women with obesity and hypertension. Archives of environmental & occupational health:1–12.

Floegel A, Drogan D, Wang-Sattler R, Prehn C, Illig T, Adamski J, et al. 2011 Reliability of serum metabolite concentrations over a 4-month period using a targeted metabolomic approach. PLoS One 6:e21103. [PubMed: 21698256]

Frederiksen M, Vorkamp K, Thomsen M, Knudsen LE. 2009 Human internal and external exposure to pbdes--a review of levels and sources. Int J Hyg Environ Health 212:109–134. [PubMed: 18554980]

Garaulet M, Perez-Llamas F, Perez-Ayala M, Martinez P, de Medina FS, Tebar FJ, et al. 2001 Site-specific differences in the fatty acid composition of abdominal adipose tissue in an obese population from a mediterranean area: Relation with dietary fatty acids, plasma lipid profile, serum insulin, and central obesity. Am J Clin Nutr 74:585–591. [PubMed: 11684525]

Gletsu-Miller N, Hansen JM, Jones DP, Go YM, Torres WE, Ziegler TR, et al. 2009 Loss of total and visceral adipose tissue mass predicts decreases in oxidative stress after weight-loss surgery. Obesity 17:439–446. [PubMed: 19219062]

Hakk H, Huwe JK, Larsen GL. 2009 Absorption, distribution, metabolism and excretion (adme) study with 2,2',4,4',5,6'-hexabromodiphenyl ether (bde-154) in male sprague-dawley rats. Xenobiotica 39:46–56. [PubMed: 19219747]

Heindel JJ, Blumberg B, Cave M, Machtinger R, Mantovani A, Mendez MA, et al. 2017 Metabolism disrupting chemicals and metabolic disorders. Reproductive toxicology 68:3–33. [PubMed: 27760374]

Helaleh M, Diboun I, Al-Tamimi N, Al-Sulaiti H, Al-Emadi M, Madani A, et al. 2018 Association of polybrominated diphenyl ethers in two fat compartments with increased risk of insulin resistance in obese individuals. Chemosphere 209:268–276. [PubMed: 29933163]

Hu X, Li S, Cirrilo P, Krigbaum N, Tran V, Ishikawa T, et al. 2019 Metabolome wide association study of serum ddt and dde in pregnancy and early postpartum. Reproductive toxicology.

Imbeault P, Chevrier J, Dewailly E, Ayotte P, Despres JP, Mauriege P, et al. 2002 Increase in plasma pollutant levels in response to weight loss is associated with the reduction of fasting insulin levels in men but not in women. Metabolism 51:482–486. [PubMed: 11912558]

Inge TH, Courcoulas AP, Jenkins TM, Michalsky MP, Helmrath MA, Brandt ML, et al. 2016 Weight loss and health status 3 years after bariatric surgery in adolescents. N Engl J Med 374:113–123. [PubMed: 26544725]

Iszatt N, Stigum H, Verner MA, White RA, Govarts E, Murinova LP, et al. 2015 Prenatal and postnatal exposure to persistent organic pollutants and infant growth: A pooled analysis of seven european birth cohorts. Environmental health perspectives 123:730–736. [PubMed: 25742056]

Jackson E, Shoemaker R, Larian N, Cassis L. 2017 Adipose tissue as a site of toxin accumulation. Compr Physiol 7:1085–1135. [PubMed: 28915320]

Johnson WE, Li C, Rabinovic A. 2007 Adjusting batch effects in microarray expression data using empirical bayes methods. Biostatistics 8:118–127. [PubMed: 16632515]

Karlsen M, Grandjean P, Weihe P, Steuerwald U, Oulhote Y, Valvi D. 2017 Early-life exposures to persistent organic pollutants in relation to overweight in preschool children. Reproductive toxicology 68:145–153. [PubMed: 27496715]

Kim KS, Lee YM, Kim SG, Lee IK, Lee HJ, Kim JH, et al. 2014 Associations of organochlorine pesticides and polychlorinated biphenyls in visceral vs. Subcutaneous adipose tissue with type 2 diabetes and insulin resistance. Chemosphere 94:151–157. [PubMed: 24161582]

Kim MJ, Marchand P, Henegar C, Antignac JP, Alili R, Poitou C, et al. 2011 Fate and complex pathogenic effects of dioxins and polychlorinated biphenyls in obese subjects before and after drastic weight loss. Environmental health perspectives 119:377–383. [PubMed: 21156398]

Le Cao KA, Gonzalez I, Dejean S. 2009 Integromics: An r package to unravel relationships between two omics datasets. Bioinformatics 25:2855–2856. [PubMed: 19706745]

Lee DH, Lind PM, Jacobs DR Jr., Salihovic S, van Bavel B, Lind L 2011 Polychlorinated biphenyls and organochlorine pesticides in plasma predict development of type 2 diabetes in the elderly: The prospective investigation of the vasculature in uppsala seniors (pivus) study. Diabetes care 34:1778–1784. [PubMed: 21700918]

Lee DH, Lind L, Jacobs DR Jr., Salihovic S, van Bavel B, Lind PM. 2012 Associations of persistent organic pollutants with abdominal obesity in the elderly: The prospective investigation of the vasculature in uppsala seniors (pivus) study. Environ Int 40:170–178. [PubMed: 21835469]

Lee DH, Porta M, Jacobs DR Jr., Vandenberg LN. 2014 Chlorinated persistent organic pollutants, obesity, and type 2 diabetes. Endocrine reviews 35:557–601. [PubMed: 24483949]

Li S, Park Y, Duraisingham S, Strobel FH, Khan N, Soltow QA, et al. 2013 Predicting network activity from high throughput metabolomics. PLoS computational biology 9:e1003123. [PubMed: 23861661]

Lichtblau Y, Zimmermann K, Haldemann B, Lenze D, Hummel M, Leser U. 2017 Comparative assessment of differential network analysis methods. Brief Bioinform 18:837–850. [PubMed: 27473063]

Lin E, Davis SS, Srinivasan J, Sweeney JF, Ziegler TR, Phillips L, et al. 2009 Dual mechanism for type-2 diabetes resolution after roux-en-y gastric bypass. The American surgeon 75:498–502; discussion 502–493. [PubMed: 19545098]

Linares V, Perello G, Nadal M, Gomez-Catalan J, Llobet JM, Domingo JL. 2010 Environmental versus dietary exposure to pops and metals: A probabilistic assessment of human health risks. J Environ Monit 12:681–688. [PubMed: 20445857]

Lynch CJ, Adams SH. 2014 Branched-chain amino acids in metabolic signalling and insulin resistance. Nat Rev Endocrinol 10:723–736. [PubMed: 25287287]

Matsusue K, Ishii Y, Ariyoshi N, Oguri K. 1999 A highly toxic coplanar polychlorinated biphenyl compound suppresses δ5 and δ6 desaturase activities which play key roles in arachidonic acid synthesis in rat liver†. Chemical research in toxicology 12:1158–1165. [PubMed: 10604864]

Meironyte Guvenius D, Bergman A, Noren K. 2001 Polybrominated diphenyl ethers in swedish human liver and adipose tissue. Arch Environ Contam Toxicol 40:564–570. [PubMed: 11525501]

Michalsky MP, Inge TH, Jenkins TM, Xie C, Courcoulas A, Helmrath M, et al. 2018 Cardiovascular risk factors after adolescent bariatric surgery. Pediatrics 141.

Murphy RA, Yu EA, Ciappio ED, Mehta S, McBurney MI. 2015 Suboptimal plasma long chain n-3 concentrations are common among adults in the united states, nhanes 2003–2004. Nutrients 7:10282–10289. [PubMed: 26690213]

Myrmel LS, Fjaere E, Midtbo LK, Bernhard A, Petersen RK, Sonne SB, et al. 2016 Macronutrient composition determines accumulation of persistent organic pollutants from dietary exposure in adipose tissue of mice. J Nutr Biochem 27:307–316. [PubMed: 26507541]

Nie C, He T, Zhang W, Zhang G, Ma X. 2018 Branched chain amino acids: Beyond nutrition metabolism. International journal of molecular sciences 19.

Panunzi S, Carlsson L, De Gaetano A, Peltonen M, Rice T, Sjostrom L, et al. 2016 Determinants of diabetes remission and glycemic control after bariatric surgery. Diabetes care 39:166–174. [PubMed: 26628418]

Pestana D, Faria G, Sa C, Fernandes VC, Teixeira D, Norberto S, et al. 2014 Persistent organic pollutant levels in human visceral and subcutaneous adipose tissue in obese individuals--depot differences and dysmetabolism implications. Environ Res 133:170–177. [PubMed: 24949816]

Ruiz D, Becerra M, Jagai JS, Ard K, Sargis RM. 2018 Disparities in environmental exposures to endocrine-disrupting chemicals and diabetes risk in vulnerable populations. Diabetes care 41:193–205. [PubMed: 29142003]

Ryder JR, Kaizer AM, Jenkins TM, Kelly AS, Inge TH, Shaibi GQ. 2019 Heterogeneity in response to treatment of adolescents with severe obesity: The need for precision obesity medicine. Obesity 27:288–294. [PubMed: 30677258]

Salihovic S, Ganna A, Fall T, Broeckling CD, Prenni JE, van Bavel B, et al. 2015 The metabolic fingerprint of p,p'-dde and hcb exposure in humans. Environment international 88:60–66. [PubMed: 26720637]

Schymanski EL, Jeon J, Gulde R, Fenner K, Ruff M, Singer HP, et al. 2014 Identifying small molecules via high resolution mass spectrometry: Communicating confidence. Environmental science & technology 48:2097–2098. [PubMed: 24476540]

Scorletti E, Byrne CD. 2013 Omega-3 fatty acids, hepatic lipid metabolism, and nonalcoholic fatty liver disease. Annual review of nutrition 33:231–248.

Soltow QA, Strobel FH, Mansfield KG, Wachtman L, Park Y, Jones DP. 2013 High-performance metabolic profiling with dual chromatography-fourier-transform mass spectrometry (dc-ftms) for study of the exposome. Metabolomics 9:S132–S143. [PubMed: 26229523]

Uppal K, Soltow QA, Strobel FH, Pittard WS, Gernert KM, Yu T, et al. 2013 Xmsanalyzer: Automated pipeline for improved feature detection and downstream analysis of large-scale, non-targeted metabolomics data. BMC bioinformatics 14:15. [PubMed: 23323971]

Uppal K, Ma C, Go YM, Jones DP. 2018 Xmwas: A data-driven integration and differential network analysis tool. Bioinformatics 34:701–702. [PubMed: 29069296]

Vafeiadi M, Georgiou V, Chalkiadaki G, Rantakokko P, Kiviranta H, Karachaliou M, et al. 2015 Association of prenatal exposure to persistent organic pollutants with obesity and cardiometabolic traits in early childhood: The rhea mother-child cohort (crete, greece). Environmental health perspectives 123:1015–1021. [PubMed: 25910281]

Vafeiadi M, Roumeliotaki T, Chalkiadaki G, Rantakokko P, Kiviranta H, Fthenou E, et al. 2017 Persistent organic pollutants in early pregnancy and risk of gestational diabetes mellitus. Environ Int 98:89–95. [PubMed: 27743729]

Valvi D, Mendez MA, Martinez D, Grimalt JO, Torrent M, Sunyer J, et al. 2012 Prenatal concentrations of polychlorinated biphenyls, dde, and ddt and overweight in children: A prospective birth cohort study. Environmental health perspectives 120:451–457. [PubMed: 22027556]

Valvi D, Mendez MA, Garcia-Esteban R, Ballester F, Ibarluzea J, Goni F, et al. 2014 Prenatal exposure to persistent organic pollutants and rapid weight gain and overweight in infancy. Obesity 22:488–496. [PubMed: 23963708]

Valvi D, Oulhote Y, Weihe P, Dalgard C, Bjerve KS, Steuerwald U, et al. 2017 Gestational diabetes and offspring birth size at elevated environmental pollutant exposures. Environ Int 107:205–215. [PubMed: 28753482]

Walker DI, Marder ME, Yano Y, Terrell M, Liang Y, Barr DB, et al. 2019 Multigenerational metabolic profiling in the michigan pbb registry. Environ Res 172:182–193. [PubMed: 30782538]

Wolff MS, Britton JA, Teitelbaum SL, Eng S, Deych E, Ireland K, et al. 2005 Improving organochlorine biomarker models for cancer research. Cancer Epidemiol Biomarkers Prev 14:2224–2236. [PubMed: 16172236]

Yu T, Park Y, Johnson JM, Jones DP. 2009 Aplcms--adaptive processing of high-resolution lc/ms data. Bioinformatics 25:1930–1936. [PubMed: 19414529]

Zamariola N, Toledo Netto P, da Silva Franchi CA, de Camargo JLV, de Marchi MRR. 2017Quechers-based method for pesticides analysis in adipose tissue associated with rat ovaries. Journal of analytical toxicology 41:399–406. [PubMed: 28334957]

Zhao X, Han Q, Liu Y, Sun C, Gang X, Wang G. 2016 The relationship between branched-chain amino acid related metabolomic signature and insulin resistance: A systematic review. J Diabetes Res 2016:2794591. [PubMed: 27642608]

Zong G, Valvi D, Coull B, Goen T, Hu FB, Nielsen F, et al. 2018 Persistent organic pollutants and risk of type 2 diabetes: A prospective investigation among middle-aged women in nurses' health study ii. Environ Int 114:334–342. [PubMed: 29477570]

Highlights

- We measured persistent organic pollutants (POPs) in tissues of severely obese adolescents
- DDE was the POP with the highest concentration in adipose tissue, and PBDE-154 had the highest concentration in liver
- Most pollutants had higher concentrations in adipose tissue than in liver
- The tissue-specific POPs burden was associated with plasma metabolic pathways

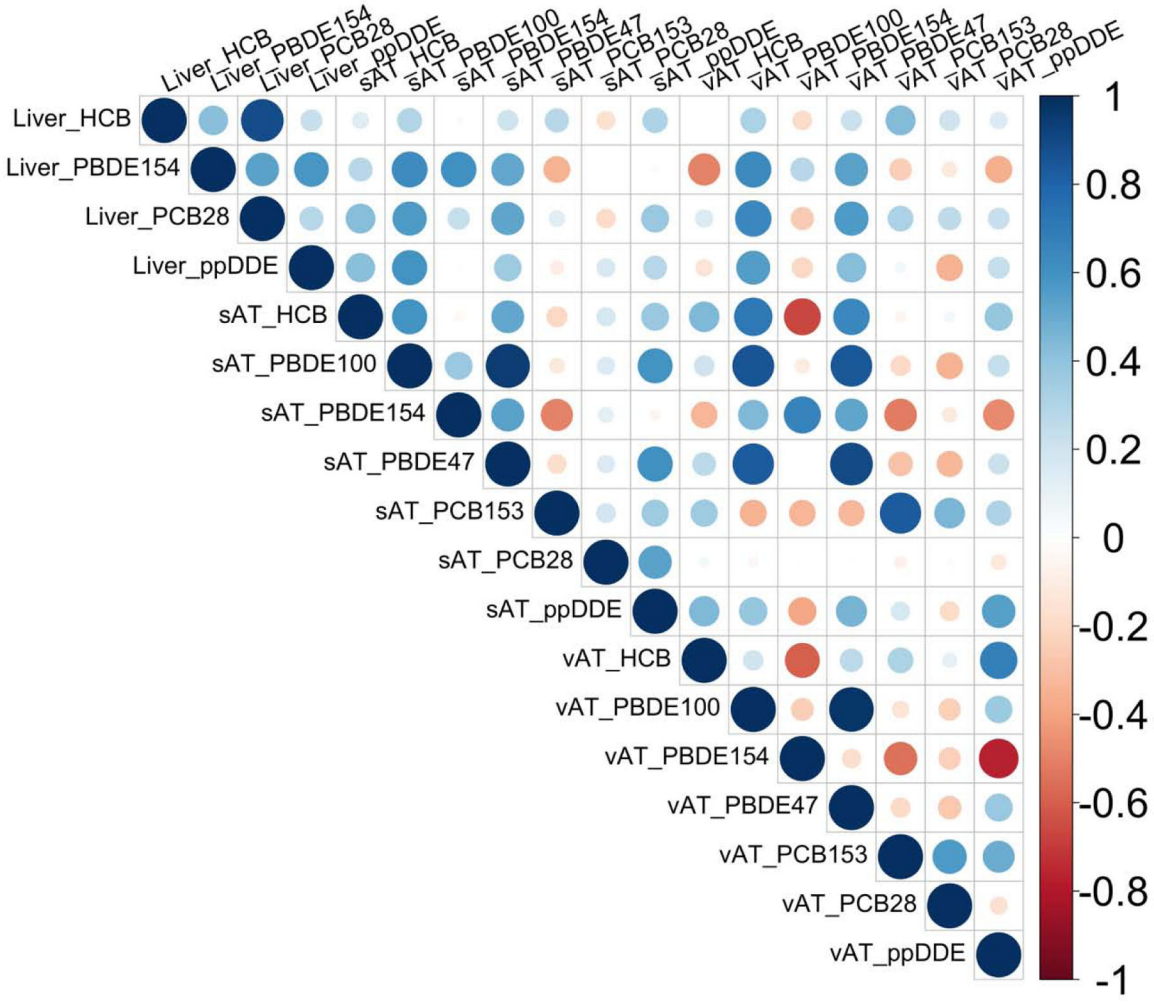

Figure 1. Between- and within-tissue correlation matrix (Spearman ρ) for pairs of POP with detection rates in metabolic tissues >80%.

Blue represents positive correlations and red negative correlations. The magnitude of the correlation coefficient is proportional to color intensity and diameter.

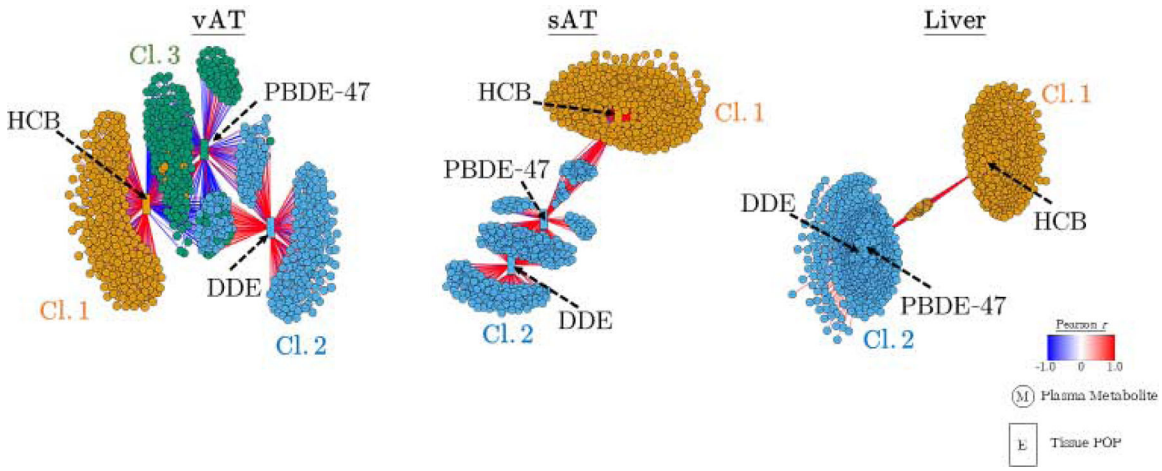

Figure 2. Plasma metabolome wide association study (MWAS) for the three POP most frequently detected in vAT, sAT and liver tissues.

Metabolites were first tested for association with each POP; clusters were identified using a multilevel community detection to identify communities of nodes that are tightly connected with each other, but sparsely connected with the rest of the network.

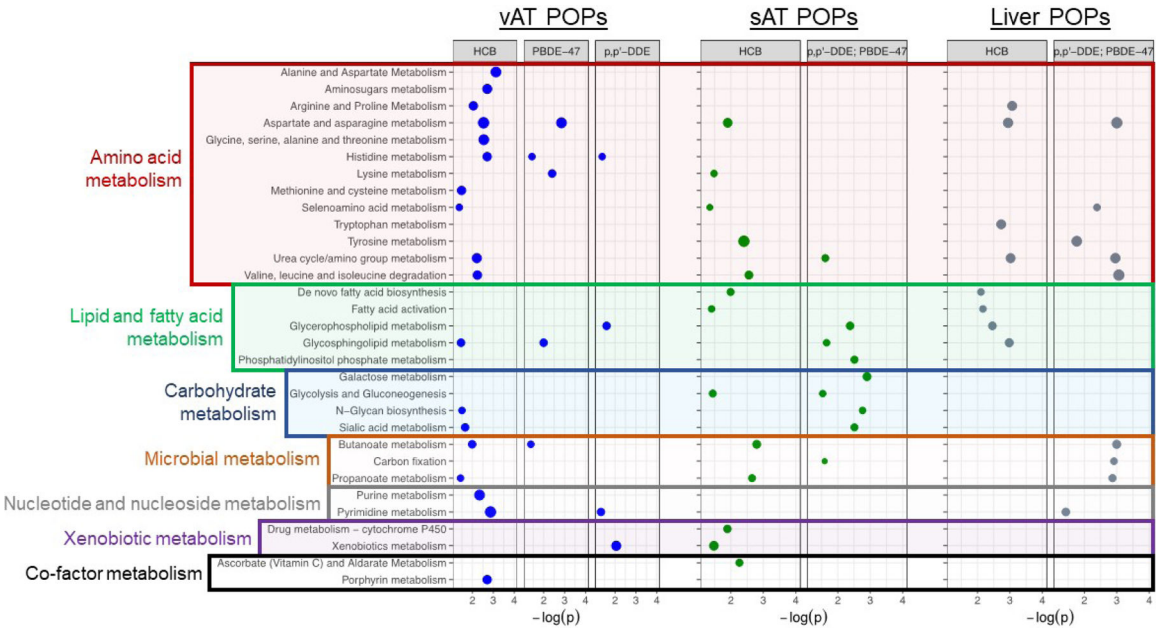

Figure 3. Metabolic pathways correlated with tissue-specific POP clusters from the plasma metabolome wide association study (MWAS).

The vertical axis represents the pathways correlated with POPs in vAT (blue circles), sAT (green circles) or Liver (grey circles). Circle radius is proportional to the number of correlated metabolite features within each pathway. The horizontal axis represents the negative $\log_{10}$ (p-value) of each pathway.

Table 1.

Detection rates and concentrations of quantifiable POPs in metabolic tissues.

Tissue	Organochlorine compounds (OCs) (pg/g-tissue)				Polybrominated diphenyl ethers (pg/g-tissue)		
	p,p'-DDE	**HCB**	**PCB-28**	**PCB-153**	**PBDE-47**	**PBDE-100**	**PBDE-154**
vAT (pg/g-tissue)							
LOD values (mean [min, max])	61 [25, 122]	54 [23, 108]	46 [19, 92]	28 [12, 56]	59 [25, 118]	93 [39, 186]	171 [71, 340]
% > LOD	100%	91%	100%	91%	100%	82%	100%
Percentile 25	3997	694	143	92	1881	140	435
Median (p50)	**5645**	**888**	**168**	**202**	**3145**	**370**	**1096**
Percentile 75	6263	1113	331	326	4261	739	1810
sAT (pg/g-tissue)							
LOD values (mean [min, max])	69 [21, 121]	61 [19, 108]	52 [16, 92]	32 [9, 56]	67 [20, 118]	105 [32, 186]	193 [58, 339]
% > LOD	100%	100%	100%	91%	100%	91%	100%
Percentile 25	6433	1264	417	112	2658	160	891
Median (p50)	**9170**	**1333**	**819**	**236**	**5316**	**651**	**1311**
Percentile 75	13810	2059	1133	626	32391	5656	2347
Liver (pg/g-tissue)							
LOD values (mean [min, max])	84 [29, 174]	75 [26, 155]	63 [22, 132]	39 [13, 81]	81 [28, 169]	128 [45, 266]	234 [82, 487]
% > LOD	100%	91%	91%	27%	55%	8%	100%
Percentile 25	404	81	39	<LOD	<LOD	<LOD	750
Median (p50)	**476**	**164**	**116**	**<LOD**	**99**	**<LOD**	**1783**
Percentile 75	1013	207	404	20	287	<LOD	2668
Comparison of mean POP concentrations across tissues							
vAT vs. sAT: p-value [1]	0.004	0.003	0.004	0.041	0.004	0.021	0.182
vAT vs. Liver: p-value [1]	0.004	0.004	0.374	NA	0.004	NA	0.790
sAT vs. Liver: p-value [1]	0.003	0.003	0.004	NA	0.003	NA	0.594

[1] P-value from non-parametric Wilcoxon signed rank test.

vAT: visceral adipose tissue; sAT: subcutaneous adipose tissue; LOD: limit of detection; NA: not applicable due to % <LOD